A monolithic distributed phase shifter based on right-handed nonlinear transmission lines at 30 GHz

Huang Jie(黄 杰)[a)b)†], Zhao Qian(赵 倩)[c)], Yang Hao(杨 浩)[d)], Dong Jun-Rong(董军荣)[d)], and Zhang Hai-Ying(张海英)[d)]

[a)] *School of Engineering and Technology, Southwest University, Chongqing* 400715, *China*
[b)] *State Key Laboratory of Millimeter Waves, Nanjing* 210096, *China*
[c)] *School of Physical Science and Technology, Southwest University, Chongqing* 400715, *China*
[d)] *Institute of Microelectronics, Chinese Academy of Sciences, Beijing* 100029, *China*

(Received 25 June 2013; revised manuscript received 28 August 2013)

The epitaxial material, device structure, and corresponding equivalent large signal circuit model of GaAs planar Schottky varactor diode are successfully developed to design and fabricate a monolithic phase shifter, which is based on right-handed nonlinear transmission lines and consists of a coplanar waveguide transmission line and periodically distributed GaAs planar Schottky varactor diode. The distributed-Schottky transmission-line-type phase shifter at a bias voltage greater than 1.5 V presents a continuous 0°–360° differential phase shift over a frequency range from 0 to 33 GHz. It is demonstrated that the minimum insertion loss is about 0.5 dB and that the return loss is less than −10 dB over the frequency band of 0–33 GHz at a reverse bias voltage less than 4.5 V. These excellent characteristics, such as broad differential phase shift, low insertion loss, and return loss, indicate that the proposed phase shifter can entirely be integrated into a phased array radar circuit.

Keywords: GaAs planar Schottky diode, phase shifter, right-handed nonlinear transmission lines, monolithic microwave integrated circuit

PACS: 73.61.Ey, 85.40.−e, 84.40.Az, 84.40.DC **DOI:** 10.1088/1674-1056/22/12/127307

1. Introduction

The continuous drive to extensive applications of phased array antenna in communication satellites, phased array radar, and WLAN has led to the development of electronically variable phase shifters.[1] In most of the recent studies, different technologies are used, such as semiconductor-device-based monolithic microwave integrated circuits (MMICs),[2–4] ferroelectric,[5,6] and microelectromechanical systems (MEMS),[7] to develop compact and low-cost phase shifters. Recently, a distributed phase shifter based on right-handed nonlinear transmission lines (RH NLTLs) in which a hybrid or monolithic Schottky diode is adopted as the variable capacitance, has widely been used as a broadband analog phase shifter due to its good performance, such as low power consumption, low insertion loss, and fast switching time.[8–10] The varactor diode is an important element in the distributed phase shifter, as a nonlinear voltage variable capacitor. Considering its sharp C–V characteristic and compatibility with the standard MMIC process, the planar Schottky varactor diode (PSVD) is an appropriate candidate for the application of the monolithic RH-NLTL phase shifter. In addition, the low series resistance, high breakdown voltage, and active-area-dependent capacitance of the PSVD can be used to achieve adjustable phase shifter over a broad voltage range to meet various application requirements.

In this paper, we present a monolithic phase shifter consisting of coplanar waveguide transmission lines (CPW TLs) periodically distributed with PSVDs, of which the epitaxial material, device structure, and fabrication technology are successfully developed in the configuration of MMIC in-house; the corresponding large signal equivalent model is explored to design a 23-distributed-Schottky transmission-line-type phase shifter. The relationships between the differential phase shift and the frequency at different reversed biases, and the other relationships between the differential phase shift and the reversed bias at different frequencies are discussed in detail. Good performances, such as a low power consumption determined by PSVD reverse biased, a minimum insertion loss of 0.5 dB, and a return loss of less than −10 dB over a band of 0–33 GHz at a reverse bias voltage less than 2.5 V, are successfully obtained.

2. Basic principle based on RH NLTLs as a phase shifter

An RH NLTL unit consists of a series high-impedance transmission line of length d and a shunt varactor $C_{\rm var}$. The high-impedance transmission line can be approximated as a lumped inductance $L_{\rm R}$ and capacitance $C_{\rm R}$. Capacitance $C_{\rm var}$

*Project supported by the Fundamental Research Funds for Central Universities, China (Grant No. XDJK2013B004), the Research Fund for the Doctoral Program of Southwest University, China (Grant No. SWU111030)，and the State Key Laboratory for Millimeter Waves of Southeast University, China (Grant No. K201312).

†Corresponding author. E-mail: jiehuang@swu.edu.cn

© 2013 Chinese Physical Society and IOP Publishing Ltd

depends on the bias voltage applied to the corresponding PSVD through the transmission line (TL). In the distributed-Schottky synthetic transmission-line phase shifter, the Bragg frequency is written as[9,11]

$$f_{\mathrm{B}} = \frac{1}{\pi\sqrt{L_{\mathrm{R}}(C_{\mathrm{R}}+C_{\mathrm{var}})}}. \tag{1}$$

Owing to the fact that the frequency is very below the Bragg frequency, the periodically varactor-distributed transmission line may be used as a synthetic transmission line, whose characteristic impedance and phase velocity are voltage-dependent and expressed, respectively, as

$$Z_{\mathrm{L}} = \sqrt{\frac{L_{\mathrm{L}}}{C_{\mathrm{L}}}} = \sqrt{\frac{L_{\mathrm{R}}}{C_{\mathrm{R}}+C_{\mathrm{var}}}}, \tag{2}$$

$$V_{\mathrm{L}} = \frac{1}{\sqrt{L_{\mathrm{L}}C_{\mathrm{L}}}} = \frac{1}{\sqrt{L_{\mathrm{R}}(C_{\mathrm{R}}+C_{\mathrm{var}})}}. \tag{3}$$

At a certain given frequency, the possible maximum differential phase shift obtainable from n units is given by

$$\begin{aligned}\Delta\varphi &= n*\Delta\beta = n\frac{\omega}{\Delta V_{\mathrm{L}}} \\ &= 2\pi f n\sqrt{L_{\mathrm{R}}}\left(\sqrt{(C_{\mathrm{R}}+C_{\mathrm{var}}^{\max})}-\sqrt{(C_{\mathrm{R}}+C_{\mathrm{var}}^{\min})}\right),\end{aligned} \tag{4}$$

where the maximum obtainable differential phase is determined by the parameters of the high-impedance TL and the capacitance difference between at the tolerable maximum and at the minimum of applied voltages. Generally, the n-unit cascaded structure is used to ensure that the characteristic of the Bragg cutoff frequency is not changed and to satisfy the requirements for the maximum different phase. CPW-based NLTL is employed due to the fact that it needs no complex processes, such as via holes and back-plating, which are needed by microstrip-based NLTL and cause a limited bandwidth (up to 40 GHz) and lower performances.[12,13]

3. Design

3.1. Schottky diode design and model

The epitaxial structure of PSVD employed in our study was grown on a 350-μm semi-insulating GaAs-substrate by molecular beam epitaxy (MBE) technology. From top to bottom, the basic structure consists of a 0.6-μm-thick n-active layer doped with Si at a level of 5×10^{16} cm^{-3}, which was determined by a tradeoff between the power handling ability and the conversion efficiency, and a 1-μm-thick n^+ layer doped with 5×10^{18} cm^{-3}, which was optimized for good Ohmic contact and lower parasitical resistance.[14,15] In this paper, the PSVDs are in-house fabricated with a Schottky contact of 160 μm^2 (20 μm × 8 μm) and cathode–anode space of 4 μm; the schematic diagram and successfully developed photograph of PSVD are shown Fig. 1.

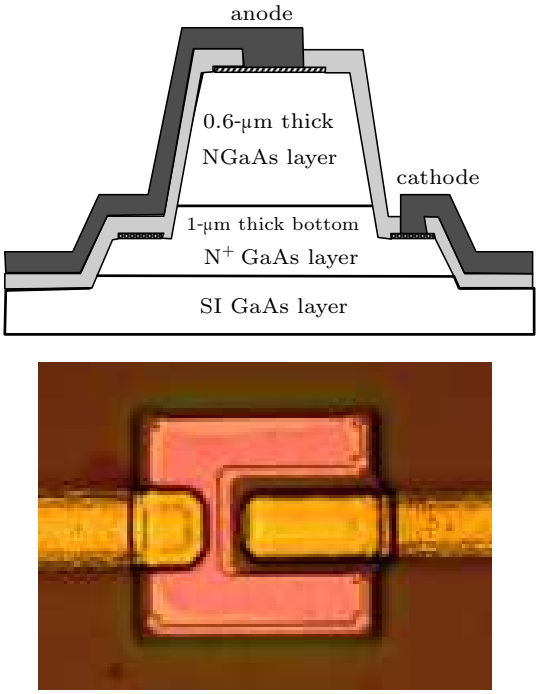


Fig. 1. (color online) Schematic diagram and photograph of PSVD.

The proposed large signal equivalent circuit model, shown in Fig. 2, is based on the fabrication process and physical layout structure of PSVD; it consists of the bias-dependent intrinsic elements and the bias-independent extrinsic elements. The intrinsic elements are composed of nonlinear junction resistance R_{j} characterized by I–V Eq. (5),

$$I = I_{\mathrm{S}}\times\left(\exp\left(\frac{V-I\times R_{\mathrm{s}}}{V_{\mathrm{T}}\times N}\right)-1\right), \tag{5}$$

where V_{T} is the thermal voltage of 25.7 mV, I_{s} is the reverse saturation current, R_{s} is the parasitic series resistance, and N is the ideality factor; also the nonlinear capacitance C_{j} by C–V Eq. (6),

$$C_{\mathrm{j}} = C_{\mathrm{j0}}/\left(1-\frac{V}{V_{\mathrm{bi}}}\right)^{M}, \tag{6}$$

where C_{j0} is the zero-bias junction capacitance, V_{bi} is the barrier potential, and M is the junction doping grading parameter. The extrinsic elements are composed of the linear series resistance R_{s}, arising from Ohmic losses in the epitaxial layer, buffer layer, metal, and the Ohmic contact, the finger-to-pad linear capacitance C_{i} and C_{o}, the pad-to-pad capacitance linear C_{p}, and the finger linear inductance L_{s}, arising from the physical geometry of PSVD.[15]

Based on the model extraction method in Ref. [16], the equivalent large signal circuit model of PSVD with a Schottky area of 160 μm^2 is proposed; it is then validated by the good agreement between the measured and modeled I–V, C–V, and S-parameters achieved up to 40 GHz under different bias conditions. Firstly, the extracted and measured capacitance–voltage characteristics for 160(20 × 8)-μm^2 PSVD at 1 MHz by an Agilent 4284 A Precision LCR Meter can be seen in

Fig. 3(a); a good agreement between them is observed. The junction capacitance of PSVD is given by Eq. (6), where C_{j0}, V_{bi}, and M are 125 fF, 0.65 V, and 0.35 respectively. The capacitance ratio between the maximum capacitance C_{max} and minimum capacitance C_{min} of PSVD over the range of applied voltages (−10 V to 0.6 V) is 5.4 and a strong nonlinearity is obtained. Secondly, the DC *I*–*V* characteristic of PSVD is measured by an HP4155 Semiconductor Parameter Analyzer. The PSVD has an extracted N of 1.0431, R_s of 3.18 Ω and I_s of 31.97 fA. Figure 3(b) shows the comparison between the measured and modeled *I*–*V* performances and their good agreement is also successfully achieved. The proposed PSVD shows a high breakdown voltage of 20 V, and then the extracted bias-independent extrinsic elements C_i, C_o, C_p, and L_s are 0.5 fF, 4 fF, 1 fF, and 10 pH, respectively. Finally the modeled *S*-parameters based on the large signal model of the PSVD shown in Fig. 2 are presented in Figs. 4(a) and 4(b), showing that they are also in excellent agreement with the measured results over the frequency range from 0.01 GHz to 40 GHz for a wide operation bias range from −10 V to 0.5 V.

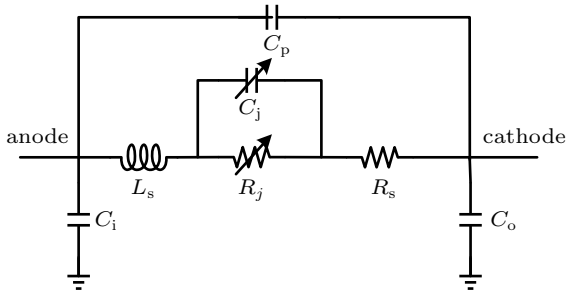


Fig. 2. Large signal equivalent circuit model for PSVD.

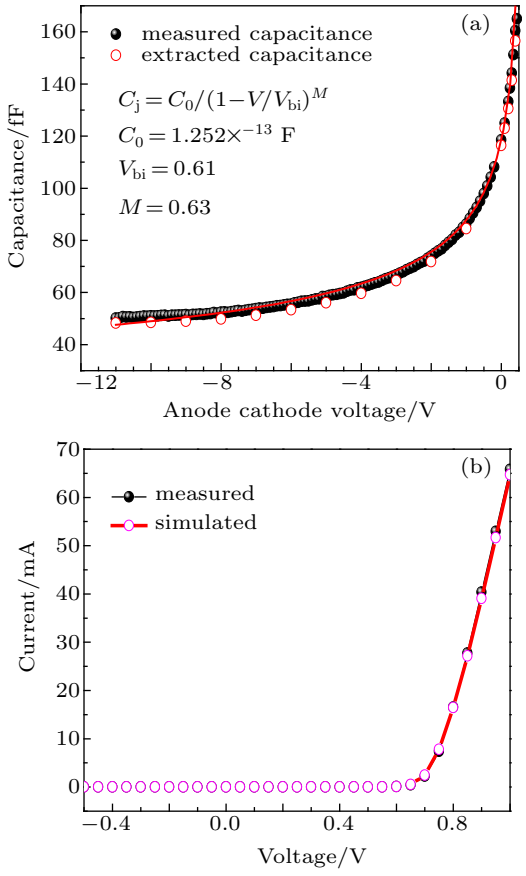


Fig. 3. (color online) Comparisons between measured and modeled dc characteristics of 160-μm^2 PSVD at different bias voltages, (a) *C*–*V*, (b) *I*–*V*.

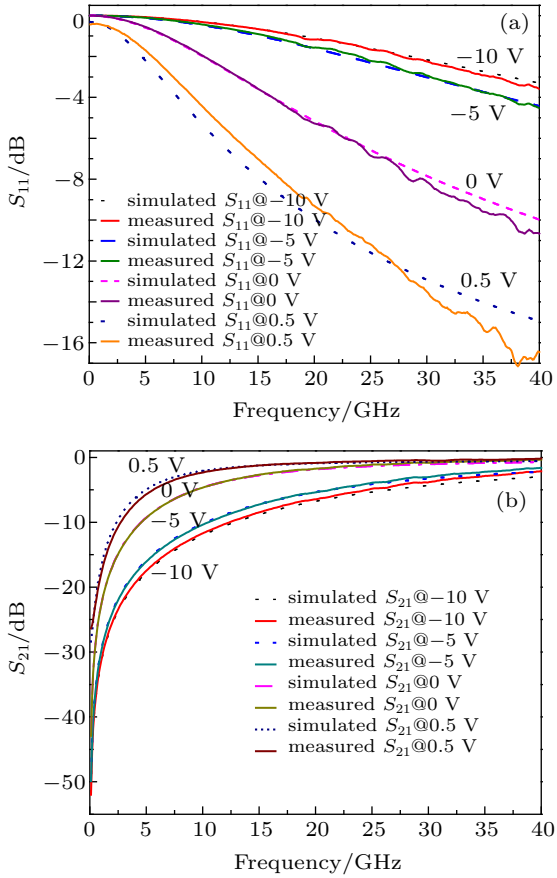


Fig. 4. (color online) Comparisons between the measured and simulated *S*-parameters of the PSVD under voltages ranging from −10 V to 0.5 V: (a) S_{11}, (b) S_{21}.

3.2. Phase shifter design

The phase shifter consists of a CPW transmission line periodically distributed by shunt PSVD. The geometric parameters of CPW TL, including the CPW conductor thickness T, the center signal line width W, the gap G between the center signal line and the ground planes sitting on each side of the center signal line, and the distance L_d between two adjacent PSVDs, are optimized to ensure that the operating frequency is a great deal below the Bragg cutoff frequency and that the insert loss and return loss are as small as possible. A symbolically defined device (SDD) model of PSVD in an Agilent advanced design system (ADS) simulator is used to de-

sign and optimize the structure parameters and number of RH NLTL units (N_t) in order to attain a continuous 0°–360° phase shift at the operating frequency above 27 GHz. Finally the obtained optimum T, W, G, L_d, and N_t are 2 μm, 20 μm, 89 μm, 300 μm, and 23, respectively. The CPW TL has a characteristic impedance of 102 Ω, and the 23-unit distributed-Schottky phase shifter has a total length of 7.16 mm. The equivalent distributed capacitance and inductance of CPW TL in an RH NLTL unit contribute to the right-handed capacitance (C_R of 0.048 pF) and inductance (L_R of 0.55 nH).[17]

4. Distributed-Schottky RH NLTL phase shifter fabrication

The phase shifter circuits were fabricated on a 350-μm semi-insulating GaAs substrate using standard GaAs processing techniques, similar to those reported in Refs. [18]–[20]. Firstly, the first mesa etching was performed to expose the buried n^+ GaAs contact layer by wet chemical etching with a solution of H_3PO_4:H_2O_2:H_2O = 2:3:30. Secondly, alloyed Ni/Ge/Au/Ge/Ni/Au Ohmic metal contacts were formed. The Schottky contacts were defined by evaporating Ti/Pt/Au and lift-off processes, then the second mesa etching was followed to achieve electronic isolation and the PSVD was passivated with 0.3-μm Si_3N_4. Then reactive ion etching was used to open windows over the metal contacts. Finally electroplating was executed to form the interconnection and CPW TL. The fabricated 23-unit distributed-Schottky phase shifters on RH NLTLs with a total length of 7.16 mm and the corresponding equivalent circuit presentation are shown in Figs. 5(a) and 5(b), respectively. It can be found in Fig. 5(b) that the parallel capacitors C_R and C_j(V) correspond to the capacitor C_R and C_{var} shown in Eq. (6) when the small parasitic series resistance R_s of PSVD is ignored.

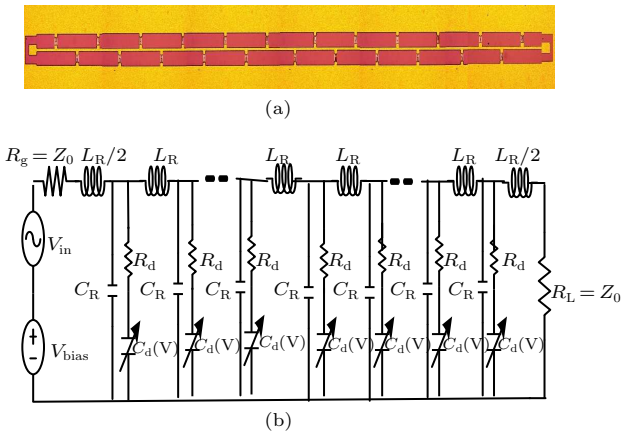


Fig. 5. (color online) (a) Fabricated phase shifters on RH NLTLs, (b) corresponding equivalent circuit model of phase shifter on RH NLTLs.

5. Measurement and discussion

The RH NLTL has normal dispersion and the frequency increases with the wave number. When the 23-unit distributed-Schottky RH NLTL phase shifter is fed by a small signal, phase shifters can be seen as a low-pass filter, which is characterized by the Bragg cutoff frequency f_B.[11] The Bragg cutoff frequency shown in Eq. (1) will decrease with the reverse voltage biased to PSVDs in the phase shifter circuit. Therefore, the operating frequency of the phase shifter under some bias voltages should be a good deal below the Bragg cutoff frequency in order to avoid a relatively large insertion loss. Theoretically, the Bragg cutoff frequencies are 32.5 GHz and 41.4 GHz for reverse bias voltages of 0 and 4.5 V, respectively.

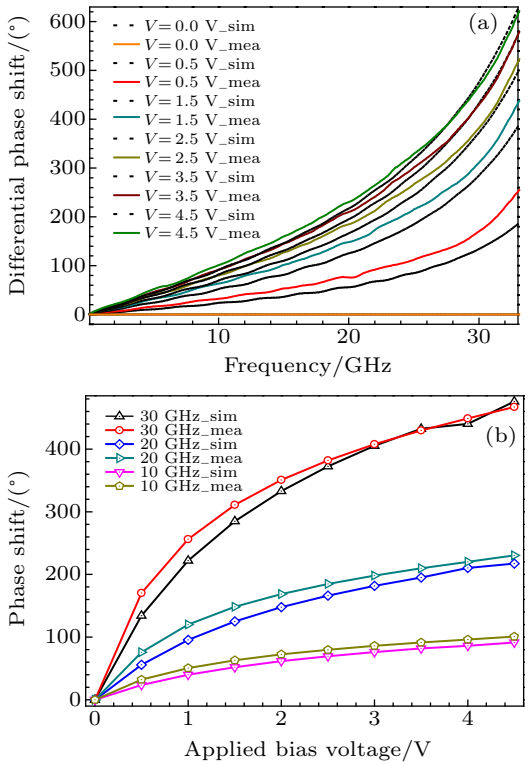


Fig. 6. (color online) (a) Plots of differential phase (arg S_{21}) versus frequency at different bias voltages and (b) the measured (mea) and simulated (sim) voltage dependences of the phase shift at frequencies of 10 GHz, 20 GHz, and 30 GHz.

The small signal measurements are taken on-wafer with an HP8510C network analyzer and a Cascade Microtech probe station using a Thru-Reflet-Line (TRL) calibration. The measured differential phase of 23-section distributed-Schottky RH NLTL phase shifters is relative to the phase at 0-V bias; it is shown in Fig. 6(a), where the reverse bias voltage increases from (bottom) 0.5 V to (top) 4.5 V in steps of 1 V. The simulated results, based on the SDD model of PSVD in Agilent ADS, are also shown for comparison; excellent agreement between their performances is obtained. The small discrepancy between them is due to the fact that the series resistance of PSVD is a function of the applied dc bias voltage, also the actual loss of CPW TL is greater than the theoretical one. Figure 6(a) shows the curves of differential phase versus the frequency for several reverse bias voltages; it can be demonstrated that the circuit is capable of realizing the continuous 0°–360° phase shift over the range from dc to 33 GHz when the reverse bias voltage applied is greater than 1.5 V. The microwave properties of phase shifters are measured from 0 V

to 4.5 V; the measured results, as a function of the voltage at a few different frequencies of 10 GHz, 20 GHz, and 30 GHz, are shown in Fig. 6(b). The phase shifter demonstrates continuous phase shifts of 0°–467°, 0°–230°, and 0°–102° over the voltage range from 0 V to 4.5 V at 30 GHz, 20 GHz, and 10 GHz, respectively. Apparently, the measured results are in good agreement with the results predicted by the SDD model, which further confirms that the model of PSVD is accurate and can be used in the other microwave circuits.

Additionally, the on-wafer *S*-parameter measurement of the phase shifter is performed from 0.1 GHz to 33 GHz at reverse bias voltages of 2.5 V, 3.5 V, and 4.5 V; their corresponding insertion losses and return losses are shown in Figs. 7(a) and 7(b), where the minimum insertion loss of the phase shifter is about 0.5 dB at a reverse bias voltage of 2.5 V and the input return loss is less than −10 dB over the frequency band from 0 to 33 GHz. The PSVD is an important element in the distributed-Schottky RH NLTL phase shifter; such small insertion loss is entirely due to the smaller series parasitic resistance R_s (3.18 Ω) of PSVD.

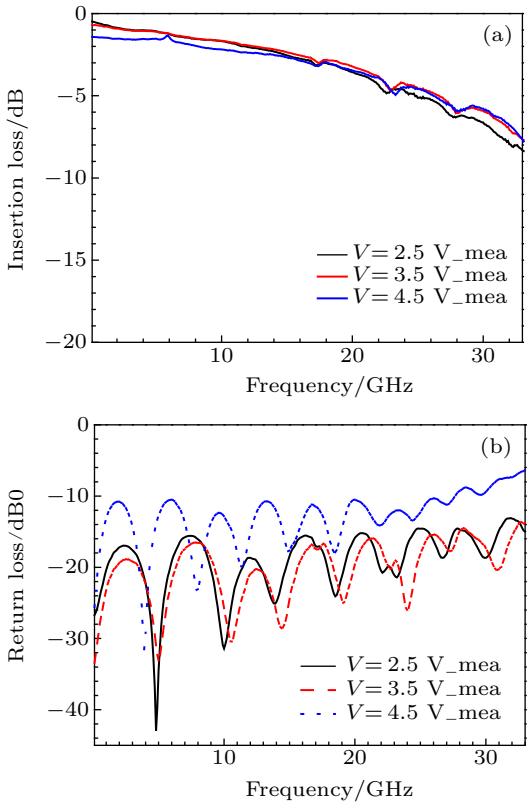


Fig. 7. (color online) Measured frequency responses of the phase shifter at reverse bias voltages of 2.5 V, 3.5 V, and 4.5 V: (a) insertion loss, (b) return loss.

6. Conclusions

A GaAs PSVD and the corresponding equivalent large signal circuit model are successfully developed to design and fabricate a distributed-Schottky phase shifter based on 23-unit RH NLTLs at 30 GHz. The simulation and measurement of the distributed-Schottky RH NLTLs phase shifter performances, such as the phase shift and *S*-parameter response, are performed and their good agreement is successfully achieved, where the simulated one is based on the SDD model of PSVD in Agilent ADS. The excellent agreement verifies the large signal equivalent model of the PSVD proposed and indicates that the model can be used in other microwave circuits. A continuous 0°–360° phase shift in a frequency range from dc to 33 GHz is achieved when the reverse bias voltage of PSVD applied is greater than 1.5 V. The PSVD with high quality, such as a small series resistance and a high breakdown voltage, results in a very small insertion loss of 0.5 dB at a reverse bias voltage of 2.5 V and an excellent return loss less than −10 dB over the frequency band of 0 GHz–33 GHz at a reverse bias voltage greater than 2.5 V. The phase shifter circuit is fabricated by the standard GaAs MMIC technology and can be integrated into other monolithic microwave integrated circuits, such as the phased array radar circuit. We believe that the phase shifter based on RH NLTLs can be further extended to the millimeter-wave frequency by reducing the Schottky active contact area of the PSVD.

References

[1] Ji T, Yoon H, Abraham J K and Varadan V K 2006 *IEEE Trans. Microwave Theory Tech.* **54** 1131
[2] Bahl I J and Conway D 2008 *IEEE Trans. Microwave Theory Tech.* **56** 293
[3] Ellinger F, Jackel H and Bachtold W 2003 *IEEE Trans. Microwave Theory Tech.* **51** 1135
[4] Chen C L, Courtney W E, Mahoney L J, Manfra M J, Chun A and Atwater H A 1987 *IEEE Trans. Microwave Theory Tech.* **35** 315
[5] Tang H J, Yang C R, Zhang J H, Chen H W, Yu A, He W and Liao Y 2010 *J. Infrared Milli. Terahz. Waves* **31** 852
[6] Suherman P M, Jackson T J, Tse Y Y, Jones I P, Chakalova R I, Lancaster M J and Porch A 2006 *J. Appl. Phys.* **99** 104101
[7] Barker N S and Rebeiz G M 2000 *IEEE Trans. Microwave Theory Tech.* **48** 1957
[8] Nagra A S, Xu J, Erker E and York R A 1999 *IEEE Trans. Microwave Guid. Wave Lett.* **9** 31
[9] Nagra A S and York R A 1999 *IEEE Trans. Microwave Theory Tech.* **47** 1705
[10] Kim H, Kozyrev A B, Karbassi A and Van der Weide D W 2007 *IEEE Trans. Microwave Theory Tech.* **55** 571
[11] Kim H, Ho S J, Choi M K, Kozyrev A B and Van der Weide D W 2006 *IEEE Trans. Microwave Theory Tech.* **54** 4178
[12] Salameh D and Linton D 1999 *IEEE Trans. Microwave Theory Tech.* **47** 1118
[13] Fernandez M, Delos E, Melique X, Arscott S and Lippens D 2001 *IEEE Trans. Microwave Wireless Compon. Lett.* **11** 498
[14] Chen S W, Ho C T, Pande K and Rice P D 1993 *IEEE Trans. Microwave Theory Tech.* **41** 2317
[15] Qun X 2005 "Millimeter and Sub-millimeter Wave Heterostructure Barrier Varactor Frequency Multipliers" (Ph. D. dissertation) (Virginia: University of Virginia) (in USA)
[16] Dong J R, Yang H, Tian C, Huang J and Zhang H Y 2012 *Chin. Phys. B* **21** 067303
[17] Wark J W R, Masayuki K, Ruai Y, Michael C, Eric C and Kirk S G 1991 *IEEE Trans. Microwave Theory Tech.* **39** 1194
[18] Huang J, Yang H, Tian C, Dong J R, Zhang H Y and Guo T Y 2010 *Chin. Phys. B* **19** 127203
[19] Bai Y, Jia R, Wu D Q, Jin Z and Liu X Y 2013 *Chin. Phys. B* **22** 027202
[20] Li H O, Huang W, Tang C W, Deng X F and Lau K M 2011 *Chin. Phys. B* **20** 068502